Realtime 2-D DOA Estimation using Phase-Difference Projection (PDP)

Hui Chen, Tarig Ballal, Xing Liu and Tareq Y. Al-Naffouri
Computer, Electrical and Mathematical Science & Engineering
King Abdullah University of Science and Technology (KAUST), Thuwal, 23955-6900
Email: {hui.chen; tarig.ahmed; xing.liu; tareq.alnaffouri}@kaust.edu.sa

***Abstract*—Estimating the direction of arrival (DOA) information of a signal is important for communications, localization and navigation systems. Time-delay based methods are popular DOA algorithms that can estimate DOA with a minimal number of receivers. Time delay can be measured with subsample accuracy using phase-difference based methods. Phase-wrapping represents a major challenge for time delay estimation that occurs when inter-sensor spacing is large. Several methods exist for phase-unwrapping; the most successful methods are those search methods, which are time-consuming and do not lend themselves to theoretical analysis. In this paper, we present a phase-difference projection (PDP) method for DOA estimation which is capable of delivering more accurate results with reduced computational complexity. The proposed method has been tested and compared with several benchmark algorithms in both simulations and experiments. The results show that, at a signal-to-noise ratio (SNR) of -18 dB, using the proposed PDP algorithm, the percentage of the DOA estimates with errors smaller than $< 5^{o}$ is 54%, and it reaches 100% at SNR = -7 dB. This performance is not matched by the benchmark methods. For the utility test, we implemented this algorithm to realize an ultrasound-based air-mouse and it achieves satisfactory user experiences when using Google Maps, or playing some interactive games.**

I. Introduction

Direction of arrival information of a target is essential in applications such as object tracking [1], communication [2], wireless sensor network (WSN) localization [3], gesture recognition [4], acoustic event detection [5], and so on. Direction-of-arrival (DOA) algorithms aim to estimate the direction a signal observed by multiple sensors on a receiver array. A summary of popular DOA algorithms can be found in [6]. The list includes popular algorithms such as beamforming [7], MUSIC [8] and ESPRIT [9]. These methods work very well when the number of sensors in the array is large. However, for applications such as indoor localization, gesture recognition, asset tracking, it is desirable to perform the localization task using minimal infrastructure. As such performance degradation is expected to occur since only a few number of receivers are employed. On the other hand, there are DOA algorithms such as PSO (particle swarm optimization) [10] that work well for small arrays but demand high computational resources.

Phase-difference based time-delay methods for DOA estimation offer accurate source localization using small receiver configurations with moderate computational cost [11]–[15]. To achieve the required level of estimation accuracy using an array of as small as two sensors dictates that the sensors be widely spaced such that the distance between two sensors is larger than $\lambda/2$ or even λ–the wavelength of the signal frequency under consideration. This results in the phase-wrapping problem.

This problem can be solved by implementing spatial-diversity based algorithms [12], [16] or frequency-diversity based algorithms [11] [17]. In our previous work [4], a DOA estimation method is proposed to estimate DOA using two receivers only. An exhaustive grid search approach is adopted to find the DOA that best matches the wrapped phase observations. This method has been accelerated by using random ferns [17]. Nevertheless, the algorithm remains computationally expensive for as far as low-cost devices are concerned. In addition, the algorithm suffers serious performance degradation at low SNR scenarios that are highly expected in acoustic environments.

This paper focuses on DOA estimation using phase-difference. To alleviate the problems with the current approaches, we propose a phase-difference projection (PDP) based method for DOA estimation for the single-source case. We will present the PDP algorithm for 1-D DOA estimation using two sensors and two signal frequencies. Then, we will show how to extend the method to 2-D DOA estimation and a realtime DOA estimation system will be demonstrated.

In this work we: 1) propose a novel 2-D DOA estimation algorithm for multi-frequency signals; 2) analyze the effect of different system parameters; 3) compare the proposed algorithm with two benchmark methods using both simulations and real tests; 4) realize an ultrasound-based air-mouse with the proposed PDP algorithm.

This paper is organized as follows. Sections II and III state the problem and explain the proposed PDP algorithm. Section IV analyzes the effect of noise and different system parameters. Section V describes how the simulations and experiments are carried out and discusses the results and applications. In section VI, we conclude the whole work with suggestions for future directions.

II. Observation model

An illustration of the far-field model for 1-D DOA estimation [4] is shown in Fig. 1. We will implement PDP algorithm on this simple model and then explain how our proposed algorithm can be adapted for 2-D DOA estimation. We assume that a source is emitting a signal with two

978-9-0827-9703-9/19/$31.00 ©2019 IEEE

or more frequencies that is observed at the two receivers. The relationship between the noise-free unwrapped phase-difference vector $\boldsymbol{\phi} = [\phi_1, ..., \phi_N]^T$ measured at frequency set $\mathbf{f} = [f_1, ..., f_N]^T$ can be stated as

$$\phi_i(\theta) = \frac{2\pi f_i \cos(\theta) D}{v} \quad (i = 1, ..., N), \tag{1}$$

where θ is the DOA, v is the speed of signal propagation, D is the distance between the two sensors and λ_i is the wavelength corresponding to frequency f_i.

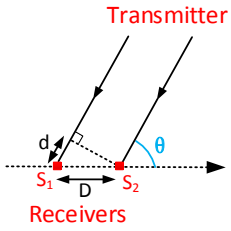

Fig. 1. 1-D DOA estimation Model.

The observed wrapped and noisy phase-difference $\hat{\boldsymbol{\psi}}$ observed between sensor 1 and sensor 2 can be derived from the received signals using [18]

$$\hat{\psi}_i = \text{ang}[Y_1(f_i)\ Y_2^*(f_i)] = \text{wrap}(\hat{\phi}_i), \tag{2}$$

where Y_1 and Y_2 are the DFT (Discrete Fourier Transform) of the received signals at sensor 1 and sensor 2, respectively, $(\cdot)^*$ indicates the complex conjugate operation, $\hat{\phi}_i$ is the noisy unwrapped phase-difference and wrap$(.)$ is the operation which limits a value to within $(-\pi, \pi]$ according to

$$\text{wrap}(\alpha) = \text{mod}(\alpha + \pi, \pi) + \pi, \tag{3}$$

where mod(a, b) returns the remainder of a divided by b.

III. DOA Estimation Using Phase-difference Observations

With the observed phase-difference vector $\hat{\boldsymbol{\psi}}$, the search based method for DOA estimation can be performed by matching $\hat{\boldsymbol{\psi}}$ with wrapped phase-differences $\psi_i(\theta_m)$ calculated for different hypothesized DOA angles θ_m $(m = 1, 2, \cdots, M)$. The final DOA estimate can be obtained by picking θ_m with the lowest mismatch [17], i.e.

$$\hat{\theta} = \arg \min_{\theta_m}\{e(\theta_m)\} = \arg \min_{\theta_m} \sum_{i=1}^{N} |\hat{\psi}_i - \psi_i(\theta_m)|. \tag{4}$$

A. Wrapped Phase-Difference Pattern (WPDP)

The search algorithm given by (4) needs to compare the observed phase-difference values with wrapped phase-difference values corresponding to the candidates in the whole angle space. In this section, we will describe the PDP algorithm, which utilizes wrapped phase differences for DOA estimation in a more efficient way. We start our development by visualizing a certain phase-difference pattern for $N = 2$. Later, we will extend the method to more than two frequencies.

Let us take as an example an acoustic signal with $\mathbf{f} = [f_1, f_2]^T = [17, 20]^T$kHz observed from a certain direction angle at a pair of receivers separated by a distance $D = 1.8$ cm. We want to verify the source location from available candidates $\theta_m \in \{20^o, 21^o, ..., 160^o\}$ (this can be changed to different ranges or increments).

In the noise-free case, each pair of wrapped phase differences $(\psi_1(\theta_m), \psi_2(\theta_m))$ calculated using (1) and (3) for various values of θ_m can be visualized as (phase-difference) point in a two-dimensional plot as represented by the blue dots in Fig. 2. Several θ_m values, such as, 105^o (1.42, 1.67), 120^o (2.75, -3.04) are highlighted in red dots. We will call such visualization a wrapped phase-difference pattern (WPDP).

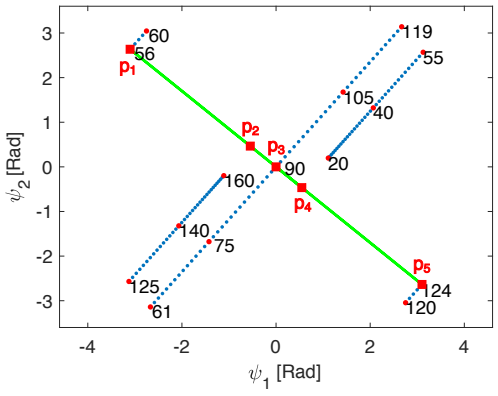

Fig. 2. An example of a wrapped phase-difference pattern.

With the increase of θ_m from 90^o to 160^o, the elements in $\boldsymbol{\phi}(\theta_m)$ will increase linearly from $(0, 0)$ to form a blue dotted line based on (1). Because $\boldsymbol{\psi}(\theta_m) = \text{wrap}(\boldsymbol{\phi})$, whenever the value in $\boldsymbol{\psi}$ reaches the boarder (π or $-\pi$), phase-wrapping takes place (e.g., from 119^o to 120^o and from 124^o to 125^o). The change of θ_m from 61^o to 60^o is in a similar way. Let us form a projection line (green solid line) across the origin point $(0, 0)$ that is perpendicular to blue lines. This line satisfies

$$\mathbf{f}^T \psi = \psi_1 f_1 + \psi_2 f_2 = 0, \tag{5}$$

where (ψ_1, ψ_2) is any point on this line.

Based on the foundations of geometry, the distance between $\boldsymbol{\psi}(\theta_m)$ and the projection line can be obtained as

$$dis[\boldsymbol{\psi}(\theta_m), \mathbf{f}^T \psi] = \frac{\mathbf{f}^T \boldsymbol{\psi}(\theta_m)}{||\mathbf{f}||}, \tag{6}$$

where $||\cdot||$ is the ℓ_2 norm. And hence the projected points (red squares) $\mathbf{p}(\theta_m)$ can be obtained as

$$\mathbf{p}(\theta_m) = \boldsymbol{\psi}(\theta_m) - \frac{\mathbf{f}^T \boldsymbol{\psi}(\theta_m)}{||\mathbf{f}||} \cdot \frac{\mathbf{f}}{||\mathbf{f}||}, \tag{7}$$

In the noise-free case, some candidates may share the same projection point (e.g., 61^o to 119^o are projected at $\mathbf{p}_3$). Given system parameters, the number K of the projection points $\mathbf{p}_k$ $(k = 1, 2, ..., K)$ can be calculated as

$$K = 2 \sum_{i=1}^{N} \text{ceil}\left(\frac{\phi_i(\theta_{max}) - \pi}{2\pi}\right) + 1 \tag{8}$$

where θ_{max} is the maximum detection DOA which equals to 160^o in this case.

The WPDP is affected by D and $\mathbf{f}$. Two illustrative examples are shown in Fig. 3 and Fig. 4 where the number next to the red square is the index of the projection point k.

In the following subsection, we show how to utilize the WPDP for DOA estimation

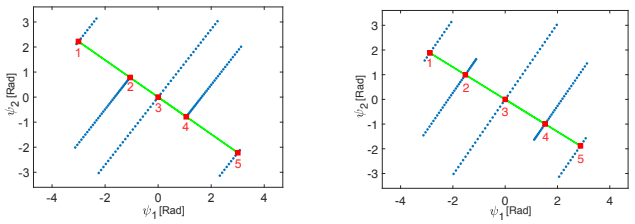

(a) f_2 = 23kHz (b) f_2 = 26kHz

Fig. 3. WPDP for different f_2 (f_1=17 kHz, D=1.8 cm).

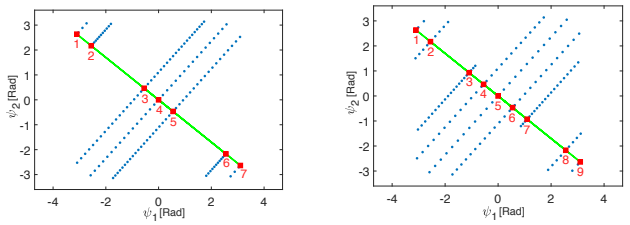

(a) D=3 cm (b) D=4 cm

Fig. 4. WPDP for different D (f_1=17 kHz, f_2=20 kHz).

B. PDP Algorithm for 1-D DOA Estimation

Phase-wrapping (or rather phase-difference wrapping) occurs when the phase value falls outside the interval $[\pi, -\pi]$ as exhibited in Fig. 2. To unwrap the phase for a pattern with K projection points, we can create an unwrapping matrix $\mathbf{U} = [\mathbf{u}_1, \mathbf{u}_2, ..., \mathbf{u}_K]$ to compensate the observed (wrapped) phase-difference. For instance, consider the pattern in Fig. 2 where $K = 5$. In this case, we have $\mathbf{u}_1 = [0, -2\pi]^T$, $\mathbf{u}_2 = [2\pi, 2\pi]^T$, $\mathbf{u}_3 = [0, 0]^T$, $\mathbf{u}_4 = [-2\pi, -2\pi]^T$ and $\mathbf{u}_5 = [0, 2\pi]^T$. In the noise-free case, for a given wrapped phase-difference pair $\boldsymbol{\psi} = [\psi_1, \psi_2]^T$, we can find the projection point using (7) and then obtain the unwrapped phase-difference vector $\boldsymbol{\phi}$ as

$$\boldsymbol{\phi} = \boldsymbol{\psi} + \mathbf{u}_k. \tag{9}$$

In other words, (9) translates the K-th line by an amount $\mathbf{u}_k$ to undo the phase-wrapping.

For an observed noisy wrapped phase-difference vector $\hat{\boldsymbol{\psi}}$, (7) returns only a perturbed projection point $\hat{\mathbf{p}}$. In this case, we choose the nearest projection point $\mathbf{p}_k$ to $\hat{\mathbf{p}}$ and then compute the unwrapped phase-difference vector $\hat{\boldsymbol{\phi}}$ using (9). Once $\hat{\boldsymbol{\phi}}$ has been estimated, we can estimate θ using (6) and (1) as

$$||\boldsymbol{\phi}(\hat{\theta})|| = \frac{\mathbf{f}^T \boldsymbol{\phi}(\hat{\theta})}{||\mathbf{f}||} = \frac{2\pi \cos(\hat{\theta}) D}{v} ||\mathbf{f}||, \tag{10}$$

and hence the DOA estimation can be obtained with

$$\cos(\hat{\theta}) = \frac{v}{2\pi D} \cdot \frac{\mathbf{f}^T \hat{\boldsymbol{\phi}}}{||\mathbf{f}||^2}. \tag{11}$$

C. 2-D DOA Estimation

The PDP algorithm described in the previous section is an effective way of estimating the 1-D DOA. In the following, we show how to obtain the 2-D DOA angles α and β in Fig. 5 (a). To this end, consider a 3-D space with a 3×1 target direction unit vector $\mathbf{t} = [\cos(\alpha), \cos(\beta), \cos(\gamma)]^T$, which we need to determine using L sensors. This creates $M = \binom{L}{2}$ distinct pairs of sensors.

Let $\mathbf{Q} = [\mathbf{q}_1, ..., \mathbf{q}_M]$ be a matrix of unit vectors of all sensor pair directions, e.g., $\mathbf{q}_i$ is the unit direction vector of the i-th sensor pair (e.g., $\mathbf{q}_1 = (S2 - S1)/||S2 - S1||$ as shown in Fig. 5 (b)). The relationship between $\mathbf{t}$ and $\mathbf{q}_i$ can be stated as

$$\cos(\theta_i) = \frac{\mathbf{q}_i^T \mathbf{t}}{|\mathbf{q}_i| \cdot |\mathbf{t}|} = \mathbf{q}_i^T \mathbf{t}, \tag{12}$$

where θ_i is obtained using PDP algorithm, which is the angle between target direction vector $\mathbf{t}$ and the i-th sensor vector $\mathbf{q}_i$. For a set of 1-D DOA estimation $\boldsymbol{\theta} = [\theta_1, ..., \theta_M]^T$, we will have

$$\cos(\boldsymbol{\theta}) = \mathbf{Q}^T \mathbf{t} = \mathbf{Q}^T [\cos(\alpha), \cos(\beta), \cos(\gamma)]^T. \tag{13}$$

where $\boldsymbol{\theta} = [\theta_1, \theta_2, ..., \theta_M]^T$. In order to have a unique solution for the unit vector $\mathbf{t}$, at least 3 non-collinear sensors are required.

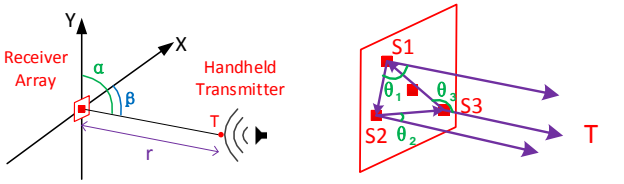

(a) 2-D DOA model (b) Sensors setup example

Fig. 5. 2-D DOA estimation model.

Although the illustrations were done for 2 frequencies, the procedure above applies for a larger number of frequencies N. Here, the only difference is the projection procedure which creates a projection hyperplane with the normal $\mathbf{f}$.

D. Summary of the Proposed PDP Algorithm

In summary, the 2-D DOA estimation using PDP algorithm can be performed in several steps as:

1. Initialize the algorithm with unwrapping matrix $\mathbf{U}$ and K projection points locations;
2. Obtain the observed phase-difference $\hat{\boldsymbol{\psi}}$ using (2);
3. Get projected point $\hat{\mathbf{p}}$ on projection line using (7);
4. Find the closest projection point $\mathbf{p}_k$ to the projected point $\hat{\mathbf{p}}$, obtain the unwrapped estimated phase $\hat{\boldsymbol{\phi}}$ using (9);
5. Calculate the direction of arrival using (11).
6. Repeat 5 for all the sensor pairs and estimate 2D DOA using (13).

IV. The Effect of Noise and Different System Parameters

A. Noise Effect

Fig.6 below is a zoom-in of the WPDP figure 4 (b). Assuming that the target's direction is $\theta = 90^o$. If the observed noisy phase-difference $\hat{\psi}$ is in the blue rectalgular area, it is guaranteed that its projected point along vector $\mathbf{f}$ on the projection line (green line) is closer to the correct projection point $k = 5$ and the error of this estimation is smaller than 1^o.

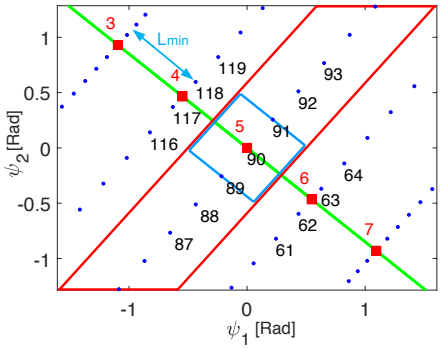

Fig. 6. Example of noise effect.

However, if $\hat{\psi}$ is out of the red area, the nearest projection point is not $k = 3$ and hence gives wrong phase compensation in the unwrapping procedure. A result is considered as a successful estimation if the corresponding projection point is correct (as shown in the red area) and otherwise, as an outlier. Assuming that the phase-difference noise is folloing a Gaussian distribution, one can easily calculate the success rate or the probability of error smaller than a certain level.

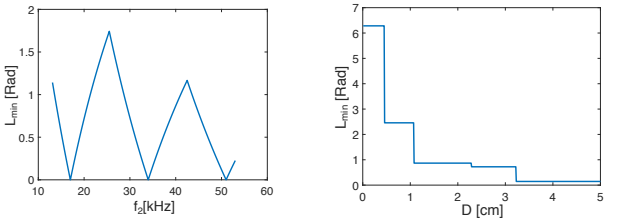

(a) f_1=20 kHz, D=1.8 cm (b) f_1=17 kHz, f_2=20 kHz

Fig. 7. Variation of L_{min} with $\mathbf{f}$ and D.

B. Effect of f and D

Accurate DOA estimation requires successful projection in the WPDP, as explained in Fig.6. We define L_{min} as the minimum distance between any two projection points

$$L_{min} = \arg \min_{<i,j>} ||\mathbf{p}_i - \mathbf{p}_j|| \qquad (i \neq j), \tag{14}$$

where $i, j \in (1, 2, ..., K)$. A large L_{min} indicates a high success rate. However, for a successful projection, the larger distance between two phase-difference points (blue dots) is expected to produce high accuracy (e.g., the result is expected to be more accurate around 90^o compared to 160^o for the same noise level). This means that D can be increased to improve the estimation as shown in Fig. 4.

The variation of L_{min} with f_2 for $f_1 = 17$ kHz and $D = 1.8$ cm, is shown in Fig. 7 (a). With the fixed $f_2 = 20$ kHz, Fig. 7 (b) shows the variation of L_{min} with D. This can be the reference for choosing $\mathbf{f}$ and D when designing a DOA system. In addition, the bandwidth of the transmitters/receivers and the channel response should also be considered.

C. The Effect of Carrier Frequency Numbers

For a certain range of the signal bandwidth, the number of frequencies will affect the value of L_{min}. Take bandwidth from 20 kHz to 23 kHz for example, the 2-D, 3-D, 4-D frequency vector can be chosen as of $\mathbf{f}_{2D} = [20, 23]$, $\mathbf{f}_{3D} = [20, 21.5, 23]$ and $\mathbf{f}_{4D} = [20, 21, 22, 23]$ (in kHz), respectively. The corresponding L_{min} for different frequency vectors are 0.6184, 0.6189, 0.6526. Compare the results with Fig. 7 we can find that the bandwidth, instead of the frequency number, has a larger effect on L_{min}. As a consequence, we will use 2 frequency components for simulation and experiment.

V. Simulation and Experimental Results

A. Simulation Results

The proposed PDP algorithm was tested both in simulation and experimentally in the real-world. We compare the PDP results with those obtained from two benchmark algorithms algorithms, namely, Grid Search [4] and Dual Freq [11]. Algorithms such as MUSIC and Capon beamformer were excluded from the final comparisons on grounds related to their unreliable performance in the considered simulation and experimental setups.

In simulation, the setup parameters were chosen as in Section III-A. The simulations were carried out for DOA in range from 1^o to 179^o with a 0.01^o increment. The simulation result of portion of the cases with error below 5^o is shown in Fig 8 (a). Instead of using RMSE as the criterion, this way of presenting results is meant to limit the impact of outliers on the conclusion of this paper.

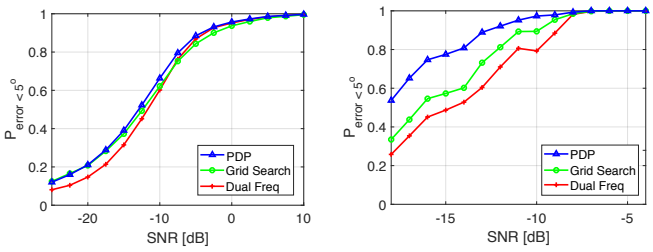

(a) Simulation results (b) Test results at 0^o DOA

Fig. 8. Simulation and experimental test results of comparing different algorithms.

From Fig 8 (a), we can see that PDP algorithm outperforms the other two algorithms when SNR > -20 dB and Dual Freq does not work well for low SNR scenario.

B. Experimental results

The experimental tests were carried out in a typical room environment with an indoor temperature of 24^oC. A pair of acoustic receivers with spacing $D = 1.8$ cm were placed horizontally at a height of 1 m above the ground. The transmitter was placed at the same height as the receivers such that its location coincided with a DOA of 90^o. The transmitter was set to periodically emit a signal of two frequencies $[17, 20]$ kHz with time duration of 2 ms duration. A sampling frequency of 96 kHz was used. By adjusting the transmitter power level, the test SNR (at the receivers) was varied from -17 dB to -4 dB.

Fig. 8 (b) depicts the percentage of estimates with error smaller than 5^o. The result showed that the proposed PDP method provides higher proportions of estimates compared to the benchmark methods.

C. Processing Time

The average processing time for one measurement of different algorithms (processed in Matlab R2018a running on a DELL T7500 workstation) is shown in Table I. We can find that the PDP algorithm is a good trade off between the processing time and algorithm performance. Its complexity is a function of K instead of the searching numbers.

TABLE I
AVERAGE PROCESSING TIME OF DIFFERENT ALGORITHMS

Algorithm	Dual Freq	Grid Search	PDP
Procesing Time [ms]	0.01	1.06	0.06

D. Utility Test

A real-time 2D DOA estimation system is realized to do utility test using a ultrasound transducer driven by an ESP32-WROOM microcontroller as shown in Fig 9. The estimation task is completed in a computer running python code processing 3-channel signals. This system is capable of completing mouse and keyboard tasks such as moving cursor, clicking, dragging, typing and air-writing. More details of using interactive applications can be found in [19].

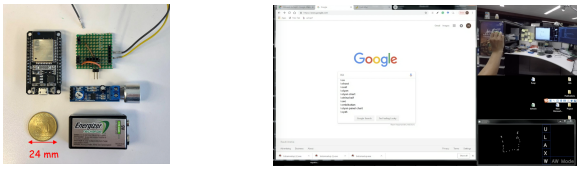

(a) Ultrasound transmitter (b) Video Screenshot

Fig. 9. Ultrasound transmitter and video screenshot.

VI. Conclusion

In this work, a phase-difference projection (PDP) based DOA algorithm was proposed. The proposed algorithm is developed by aid of a wrapped phase-difference pattern display. We discussed how different parameter choices will affect the phase-difference pattern and gave suggestions on parameter selection.

The proposed PDP algorithm was tested in both simulation and experimentally. Comparison with other benchmark methods were carried out. We conclude that the proposed PDP offers an improved performance over the benchmark methods.

References

[1] L. Wan, G. Han, L. Shu, S. Chan, and T. Zhu, "The application of doa estimation approach in patient tracking systems with high patient density," *IEEE Transactions on Industrial Informatics*, vol. 12, no. 6, pp. 2353–2364, 2016.

[2] R. Shafin, L. Liu, J. Zhang, and Y.-C. Wu, "Doa estimation and capacity analysis for 3-d millimeter wave massive-mimo/fd-mimo ofdm systems," *IEEE Transactions on Wireless Communications*, vol. 15, no. 10, pp. 6963–6978, 2016.

[3] S. Tomic, M. Beko, and R. Dinis, "3-d target localization in wireless sensor networks using rss and aoa measurements," *IEEE Transactions on Vehicular Technology*, vol. 66, no. 4, pp. 3197–3210, 2017.

[4] H. Chen, T. Ballal, M. Saad, and T. Y. Al-Naffouri, "Angle-of-arrival-based gesture recognition using ultrasonic multi-frequency signals," in *Signal Processing Conference (EUSIPCO), 2017 25th European*. IEEE, 2017, pp. 16–20.

[5] Y. Guo and M. Hazas, "Localising speech, footsteps and other sounds using resource-constrained devices," in *Information Processing in Sensor Networks (IPSN), 2011 10th International Conference on*. IEEE, 2011, pp. 330–341.

[6] M. Haardt, M. Pesavento, F. Roemer, and M. N. El Korso, "Subspace methods and exploitation of special array structures," in *Academic Press Library in Signal Processing*. Elsevier, 2014, vol. 3, pp. 651–717.

[7] V. Krishnaveni, T. Kesavamurthy, and B. Aparna, "Beamforming for direction-of-arrival (doa) estimation-a survey," *International Journal of Computer Applications*, vol. 61, no. 11, 2013.

[8] R. Schmidt, "Multiple emitter location and signal parameter estimation," *IEEE transactions on antennas and propagation*, vol. 34, no. 3, pp. 276–280, 1986.

[9] A. Paulraj, R. Roy, and T. Kailath, "Estimation of signal parameters via rotational invariance techniques-esprit," in *Circuits, Systems and Computers, 1985. Nineteeth Asilomar Conference on*. IEEE, 1985, pp. 83–89.

[10] M. Li and Y. Lu, "Angle-of-arrival estimation for localization and communication in wireless networks," in *Signal Processing Conference, 2008 16th European*. IEEE, 2008, pp. 1–5.

[11] T. Ballal and C. J. Bleakley, "Doa estimation for a multi-frequency signal using widely-spaced sensors." in *EUSIPCO*, 2010, pp. 691–695.

[12] ——, "Phase-difference ambiguity resolution for a single-frequency signal," *IEEE Signal Processing Letters*, vol. 15, pp. 853–856, 2008.

[13] C. Hekimian-Williams, B. Grant, X. Liu, Z. Zhang, and P. Kumar, "Accurate localization of rfid tags using phase difference," in *RFID, 2010 IEEE International Conference on*. IEEE, 2010, pp. 89–96.

[14] J.-F. Gu, W.-P. Zhu, and M. Swamy, "Joint 2-d doa estimation via sparse l-shaped array," *IEEE Transactions on Signal Processing*, vol. 63, no. 5, pp. 1171–1182, 2015.

[15] A. Lin and H. Ling, "Doppler and direction-of-arrival (ddoa) radar for multiple-mover sensing," *IEEE transactions on aerospace and electronic systems*, vol. 43, no. 4, 2007.

[16] T. Ballal and C. J. Bleakley, "Doa estimation of multiple sparse sources using three widely-spaced sensors," in *Signal Processing Conference, 2009 17th European*. IEEE, 2009, pp. 1978–1982.

[17] H. Chen, T. Ballal, and T. Al-Naffouri, "Fast phase-difference-based doa estimation using random ferns," in *Signal and Information Processing (GlobalSIP), 2018 IEEE Global Conference on*. IEEE, 2018.

[18] M. M. Saad, C. J. Bleakley, and S. Dobson, "Robust high-accuracy ultrasonic range measurement system," *IEEE Transactions on Instrumentation and Measurement*, vol. 60, no. 10, pp. 3334–3341, 2011.

[19] Ultrasonic air-writing demo. https://www.youtube.com/watch?v=XRi2iezsG4Q&t=2s. Accessed: 2019-03-04.